Dual-polarized Near-field Plane Wave Generator using an offset-optics reflectarray mm-Wave band

Álvaro F. Vaquero, *Member*, *IEEE*, Rafael Florencio, Marcos R. Pino, and Manuel Arrebola, *Senior Member*, *IEEE*

***Abstract*—In this work, a reflectarray antenna is presented as a dual-polarized plane wave generator (PWG) in mm-wave frequencies. The reflectarray produces a uniform plane wave within its near field in a volume close to the aperture. A dual-polarized pencil beam reflectarray is used as starting point to carry out a phase-only synthesis (POS) to reach a dual-polarized uniform plane wave. The synthesis aims to overcome the amplitude limitation due to the incident field while preserving the phase flatness. The phase distribution obtained in the POS is used to carry out a design based on sets of orthogonal-coplanar dipoles. This unit cell provides independent control of each polarization using a single-layer topology. The design is manufactured, and the prototype is measured in a planar acquisition range facility. The prototype shows discrepancies with simulation and further analysis is carried out. After finding out the proper value of the dielectric constant, a new design is carried out. The second prototype shows a good agreement with simulations, obtaining that reflectarray antennas are a suitable and low-profile solution to produce uniform plane waves within the near field.**

***Index Terms*—Dual-polarized plane wave generator, reflectarray antenna, near-field synthesis, near-field pattern.**

I. Introduction

Throughout the last decades, the most popular solution to measure the radiation pattern of an antenna is a Compact Antenna Test Range (CATR) [1]. The working principle is based on the existence of an area known as the Quiet Zone (QZ). The QZ is defined as an area within the near field of the probe wherein the field behaves like a uniform plane wave. Hence, the QZ emulates far-field conditions. In recent years, a true interest has arisen in the development of novel antenna measurement systems with the capability of performing fast evaluations of the device performance (such as directivity, pointing direction, or operational bandwidth) without needing a fixed, expensive, and bulky facility. Therefore, developing portable systems that can be fast deployed in an area of interest. Besides, the system must provide similar performance to a fixed facility but reduce both dimensions and costs.

In the literature, different alternatives have been proposed [2],[3], at mm-wave frequencies, especially for the 5G band FR2 [4]. However, most of them require a post-processing stage to finally get the radiation pattern. A potential alternative to avoid this last stage is the use of the standard Over-The-Air (OTA). OTA ideally aims to measure the Antenna Under Test (AUT) performance at an infinity distance without a direct connection to the probe [5]. Hence, carrying out the measurements in far-field conditions. At FR2, a CATR-based system is an attractive alternative since it can generate a uniform plane wave within the near-field region that can be used to evaluate the antenna performance within a short-range.

The more mature CATRs commonly used a parabolic reflector to collimate the impinging wave provided by the primary feed (typically a horn antenna). Within the near field of the collimated field, the QZ might be found. The size of the QZ depends on two factors: the antenna aperture, and the illumination taper onto the reflector surface. Thus, the QZ is improved by a large ratio f/D. The larger the focal distance, the lower the illumination taper, at the price of obtaining bulkier structures. Conversely, a lower f reduces the dimensions but it increases the illumination taper, and the QZ is affected too. A dedicated-low-directivity feed can be used to reduce both f and the illumination taper. However, the field at the edges will increase, therefore the edge diffraction increases too. Another alternative implies using a dual-reflector configuration, such as a Cassegrain or Gregorian reflector. These configurations aim to control the amplitude taper with the subreflector surface, while the phase is controlled by the main reflector. However, either a dedicated feed or a dual-reflector lead to complex and high-cost solutions, which are not suitable for compact and low-cost systems.

In the last years, plane wave generators (PWG) have been intensively studied in the literature. A PWG is defined as an array antenna that radiates a uniform plane wave within its near-field region [5], [6]. Therefore, it can be used to measure the antenna performance at a reduced distance between the AUT and the probe. However, array antennas require the design of complex feeding networks to properly control the excitation of the array elements. To overcome this issue, reflectarray antennas have been proposed to generate uniform plane waves [7]-[9]. In particular, in [10] an experimental prototype was shown for the first time. The achieved uniform plane wave satisfies the tight requirement of a maximum deviation of ± 0.5 dB and 5° in amplitude and phase, respectively. Nearly 90% of the measured planes satisfy these specifications within a volume of $100\ \text{mm} \times 100\ \text{mm} \times 150\ \text{mm}$ at 28 GHz. This prototype only works on single-linear polarization. However, in the literature, several dual-polarized reflectarray antennas have been reported for far-field applications, especially for space communications [11]-[16].

In this work, a single-layer dual-polarized reflectarray antenna is presented as a PWG for being used in a compact and portable CATR for measuring 5G new radio devices. A Phase-Only Synthesis (POS) is carried out using the generalized Intersection Approach for near-field [10],[17] to obtain a suitable phase distribution of the X- and Y-

This work was supported in part by Ministerio de Ciencia e Innovación and Agencia Española de Investigación within the project PID2020-114172RB-C21/AEI/10.13039/501100011033, and by Gobierno del Principado de Asturias within the project AYUD/2021/51706.

Á. F. Vaquero, M. R. Pino, and M. Arrebola are with the Department of Electrical Engineering, Group of Signal Theory and Communications, Universidad de Oviedo, Gijón, 33203, Spain (e-mail: {fernandezvalvaro, mpino, arrebola}@uniovi.es).

R. Florencio is with the Department of Physics and Mathematics, Universidad de Alcalá, Alcalá de Henares, 28801, Spain, (e-mail: rafael.florencio@uah.es).

.

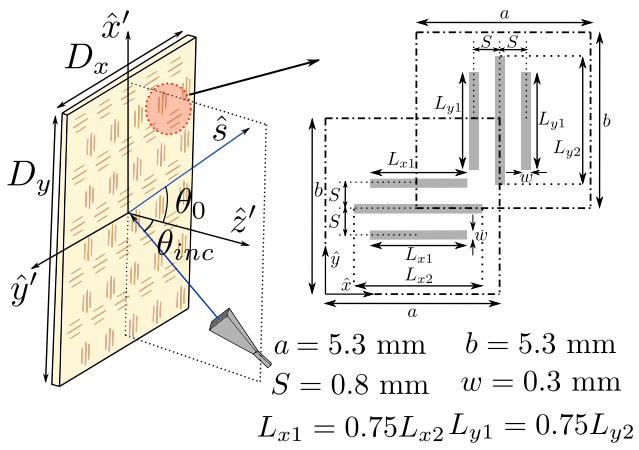

Fig. 1 Scheme of a single-offset reflectarray antenna based on an orthogonal-coplanar dipole unit cell.

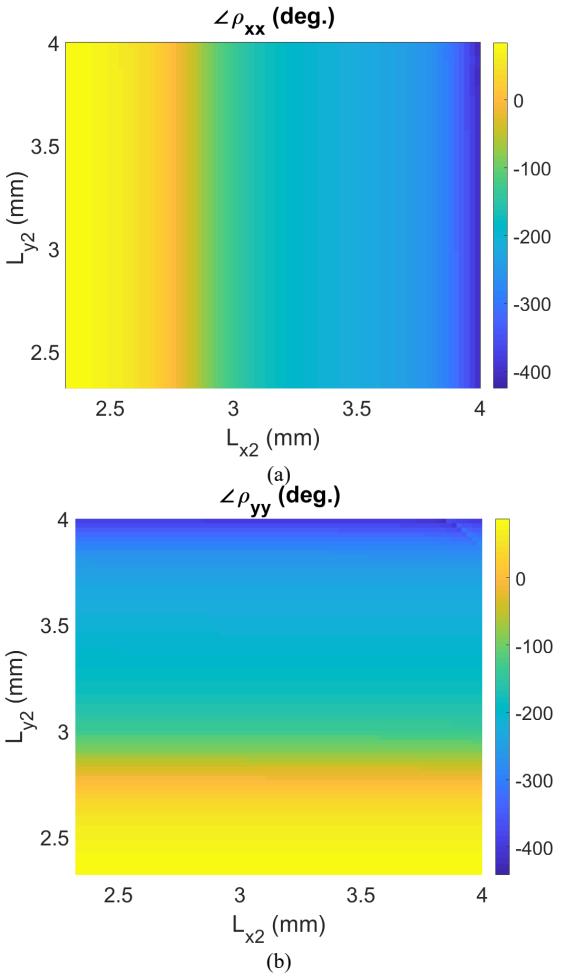

Fig. 2. Color-maps of the phase of co-polar reflection coefficients (a) ρ_{xx} and (b) ρ_{yy} obtained when the lengths, L_{x2} and L_{y2} are simultaneously varied at 28 GHz under oblique incidence given by $\theta_{\text{inc}} = \varphi_{\text{inc}} = 20°$.

polarizations. The phase distribution must ensure that the radiated near field behaves as a uniform plane wave, thus satisfying the stringent deviation requirements. Then, the reflectarray is made up of two arrays that host two orthogonal sets of three parallel dipoles, so that both polarizations are controlled by the length of the dipoles on the single layer. The prototype is designed, manufactured, and measured in a planar acquisition range. The results show discrepancies with simulations, finding out that the dielectric permittivity of the single layer ϵ_r is not properly characterized. After a further analysis a new design is done, manufacturing a new prototype that is also evaluated. This design considers the proper characterization of the dielectric permittivity. The new results shown in this paper demonstrate that reflectarray antennas are suitable candidates to control both amplitude and phase of the near-field in dual-linear polarization. Moreover, the in-band analysis shows that it is feasible to cover a 5G mm-wave channel, though the design is carried out using a POS process at a single frequency. Hence, the proposed reflectarray can be used as a probe of an easy-low-cost reflectarray-based CATR in mm-wave band.

II. Single-Layer Dual-Polarized Reflectarray Design

A. *Antenna optics and design procedure*

The reflectarray consists of a grounded-low-loss-dielectric layer of RO4003C of 0.8128 mm thickness [18], which hosts the resonant printed elements. According to the datasheet of RO4003C, two different values of the dielectric constant are recommended ($\epsilon_r = 3.38$ and $\epsilon_r = 3.55$). In this case, the design process is carried out considering an average value between both, thus $\epsilon_{r,design} = 3.45$, whereas the highest loss tangent is considered. The resonant elements are arranged in two square grids of periodicity 5.3 mm × 5.3 mm. A square grid contains 36×36 elements to control the X-polarization, while the other square grid contains 35×35 elements to control the Y-polarization. Each square grid is displaced half of a period about the other (see Fig. 1) in the orthogonal directions of the lattice. The reflectarray aperture size is 190.8×190.8 mm^2. It should be noted that both polarizations are controlled with a single-layer reflectarray, which provides an easy manufacturing process as well as a low-complexity topology of the reflectarray element. This unit cell avoids the delicate bonding process of multi-layers topologies.

According to Fig. 1, the feed is placed at $(x_f, y_f, z_f) = (-79.3, 0, 200)$ mm. The feed is a standard pyramidal horn antenna of 20 dBi gain (NARDA v639) at 28 GHz. The illumination taper at the edge of the reflectarray is about -16 dB, considering the maximum at the center of the reflectarray. The unit cell is based on a set of coplanar dipoles. Fig. 1 shows two adjacent unit cells. Each one belongs to a different square grid, and the distance between the two centers is half of a period in the x- and y-direction. The unit cell that hosts the coplanar dipoles oriented in the x-axis control the phase response of the X- polarization, while the dipoles oriented in the y-axis control the phase response of the Y-polarization. The phase response of the unit cell is controlled by the lengths of the dipoles, and to ensure a low cross-copolar level the symmetry is maintained for the dipoles, which are edge coupled to the central dipole in each unit cell [15]. The lateral dipoles of each unit cell are identical, and the distance to the central one is also the same. The other geometrical parameters are adjusted to provide a smooth and linear phase response for variations in the length of the dipoles. The unit cell is analyzed with a home-made electromagnetic code based on the Method of Moments in Spectral Domain (MoM-SD). The analysis is carried out considering the periodic environment, and base functions accounting for edge singularities are used in the approximation of the current density of the dipoles [19].

The phase of the co-polar reflection coefficients (ρ_{xx} and ρ_{yy}) and the magnitude of the cross-polar reflection coefficients (ρ_{xy} and ρ_{yx}) have been studied for oblique incidence ($\theta_{\text{inc}} = \varphi_{\text{inc}} = 20°$) at 28 GHz when the dipole lengths L_{x2} and L_{y2} are simultaneously varied. Fig. 2 shows the smooth and progressive phase variation of the ρ_{xx} and ρ_{yy}. These results show that the phase control is totally

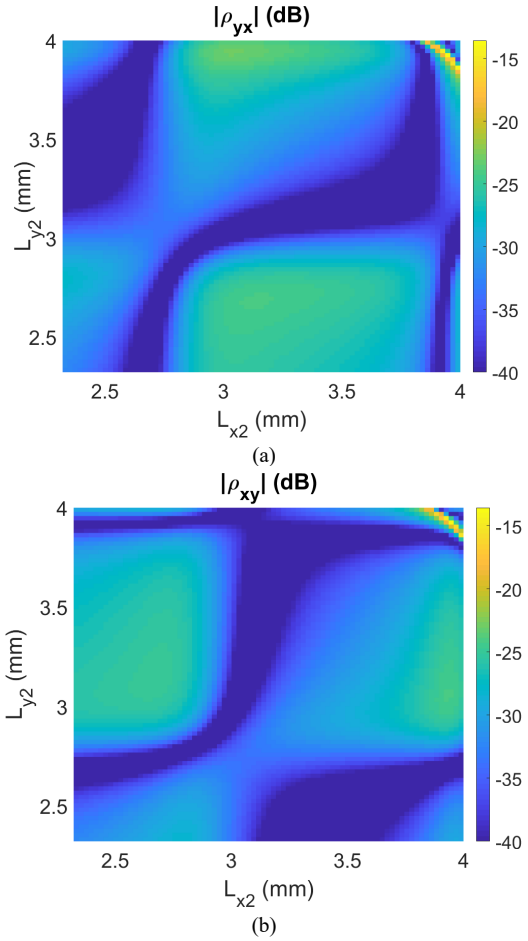

Fig. 3. Color-maps of phase of cross-polar reflection coefficients (a) ρ_{yx} and (b) ρ_{xy} obtained when when the lengths, L_{x2} and L_{y2} are simultaneously varied at 28 GHz under oblique incidence given by $\theta_{\text{inc}} = \varphi_{\text{inc}} = 20°$.

independent for both polarizations. Besides, even under oblique incidence, the obtained phase-shift is larger than a phase cycle (more than 400°). The magnitude of ρ_{xx} and ρ_{yy} is lower than 0.2 dB on average (not shown) The magnitude of ρ_{xy} and ρ_{yx} is shown in Fig. 3. The maximum and mean values are nearly 15 dB and 25 dB lower than ρ_{xx} or ρ_{yy} for most of the combinations of L_{x2} and L_{y2}. Only the area associated to the values close to $L_{x2} = L_{y2} = 4$ mm increases the magnitude values, mainly due to a spurious resonance [15]. To avoid this area in the design, a phase difference of 180° is applied between the phase shifts of each linear polarization in all the elements.

Since the unit cell provides independent control of both linear polarizations, the POS process is split into two independent processes, one for each polarization. Each process is carried out with the generalized Intersection Approach for near field [10], [17]. This approach allows considering constraints in the amplitude and phase of the radiated near field simultaneously. In this case, the maximum deviation about the average value is ±0.5 dB in amplitude and ±5° in phase, which are the standard deviation to consider that the near field behaves as a uniform plane wave.

B. Phase-Only Synthesis with amplitude and phase constraints

The starting point is the phase distribution of a pencil beam [20]. The beam points at $\theta_o = 20°$ in the direction $\hat{s}$ (see Fig. 1) for both polarizations. This starting point nearly provides a plane wave. However, the amplitude is deeply affected by the illumination taper. The uniform plane wave is evaluated in a perpendicular plane to $\hat{s}$

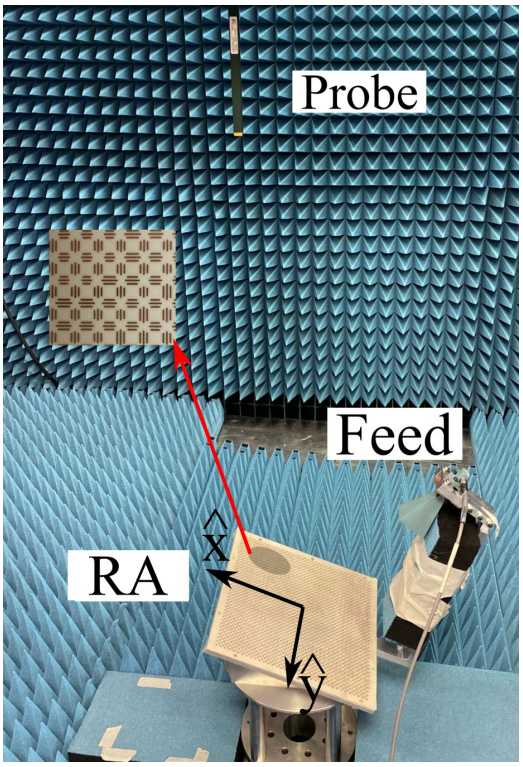

Fig. 4 Setup at the planar acquisition range of the measured prototype.

direction at 500 mm ($46.7\lambda_0$ at 28 GHz). Considering that the far-field is reached at $1170.4\lambda_0$ (i.e., 12.52 m), the overall dimension (reflectarray plus uniform plane wave) of the system is very compact. The specifications of the uniform plane wave are imposed within a circular area of diameter 100 mm (equivalent to 56.6% of the antenna aperture in the offset plane of the reflectarray).

The syntheses are divided into a multi-stage process [21]. The synthesis for the X-polarization required 9 stages, while the Y-polarization 12 stages. In each stage, synthesis is carried out using the generalized Intersection Approach, and the requirements are gradually tightened from one stage to the next one. In the first stages, it is common to use laxer requirements, i.e., ±1.5 dB and ±10° of maximum deviation. Then, the requirements are tightened until finally reaching the desired specifications. The output of these processes is the phase distribution that should introduce the elements for each polarization. Then, to avoid spurious resonances in the design (the spurious resonance close to $L_{x2} = L_{y2} = 4$ mm), a 180° shift is introduced in one of the phase distributions. Besides, having different lengths in the dipoles of one polarization about the other will increase the room for the orthogonal dipoles that are printed on the same dielectric layer.

In the design L_{x2} and L_{y2} are adjusted to produce the phase shift obtained as a result of the synthesis. Throughout the design, the other geometrical parameters remain constant. This process is carried out element-by-element, under local periodicity assumption [13], considering the real angle of incidence, and the dielectric loss in the complex permittivity of the dielectric. Every element is analyzed using a home-made electromagnetic code based on MoM-SD [11]. The output of the design process is a layout whose dipole lengths L_{x2} and L_{y2} minimize the phase error about the required phase shift. Then, a zero-finding routing [12] is used to improve the adjustment considering both polarizations simultaneously.

Table I outlines a comparison of the deviations and specifications compliance of the uniform plane wave generated by the initial pencil beam distribution, the synthesized phase distribution, and the designed

TABLE I: Evaluation of the maximum deviations with respect to average values and the specification compliance in the quiet zone for the starting phase distributions, optimized phase distributions and designed reflectarray for X- and Y-polarizations:

			Initial		Synthesized		Designed	
		Specifications	Maximum Deviation	Compliance (%)	Maximum Deviation	Compliance (%)	Maximum Deviation	Compliance (%)
X-pol.	(dB)	**[-0.5, 0.5]**	**-5.51**	**16.84**	**-0.26**	**100**	**-0.19**	**100**
	(deg.)	**[-5, 5]**	**-7.81**	**88.00**	**-11.76**	**79.60**	**-14.79**	**82.64**
Y-pol.	(dB)	**[-0.5, 0.5]**	**-4.36**	**16.69**	**0.35**	**100**	**0.39**	**100**
	(deg.)	**[-5, 5]**	**-10.16**	**69.91**	**7.06**	**79.65**	**7.92**	**95.16**

reflectarray at 28 GHz. According to these results, the compliance in amplitude is notably improved by the synthesis in both polarizations. A poor 16.7% of the starting radiated near-field is within an amplitude deviation of ±0.5 dB, whereas 100% is reached after the synthesis. Besides, the maximum deviation is reduced by more than 4 and 5 dB in both polarizations. These results are obtained at the cost of barely increasing the phase ripple in the X-polarization. However, the phase compliance is still high since almost 80% of the phase is within ±5° deviation. This compliance is slight improved in the designed reflectarray. This slightly difference is mainly associated with the material and the real angle of incidence is considered in the computation of the reflection coefficients due to the MoM-SD used in the design process.

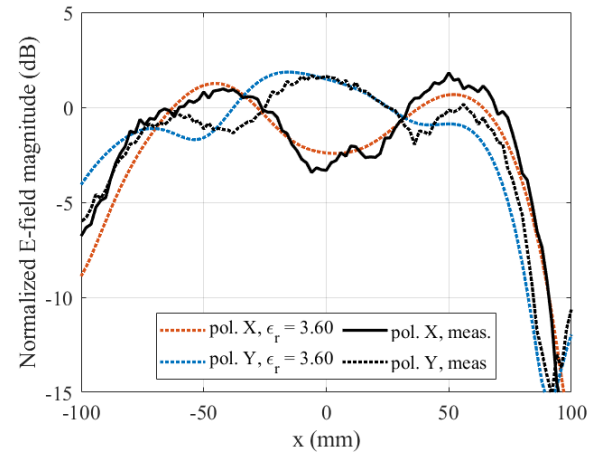

(a)

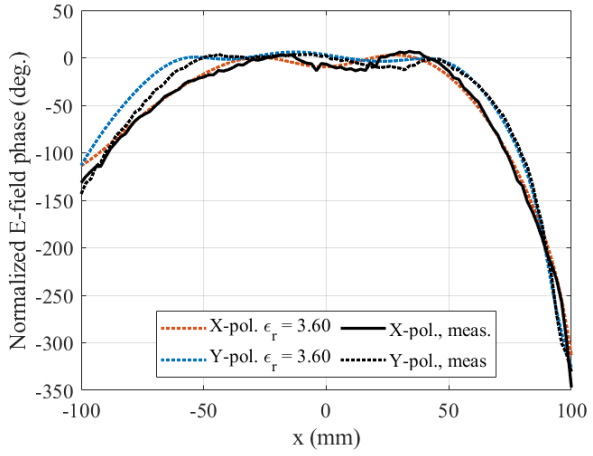

(b)

Fig. 5. Comparison of the normalized (a) amplitude and (b) phase of the electric field in the main cut $y = 0$ of the uniform plane wave for the simulations carried out considering a dielectric constant of $\epsilon_r = 3.60$ and measurements.

III. Experimental validation

The designed reflectarray is manufactured and evaluated in the planar acquisition range at the University of Oviedo. The prototype and the setup are shown in Fig. 4. The reflectarray is placed on an aluminum structure tilted 20° so that the uniform plane wave is parallel to the probe aperture (an open-ended Ka-band waveguide). The uniform plane wave is measured at 500 mm through a volume of $50 \times 50 \times 150$ mm^3 at 28 GHz.

A. Dielectric constant correction

The measured amplitude and phase are shown in Fig. 5 for both polarizations at the main cuts ($x = 0$ and $y = 0$). The amplitude is normalized to the average value of the whole plane. The measured amplitude shows a ripple of 3 dB and 2 dB for the X- and Y-polarization, respectively. The maximum distortion in the amplitude is found at the center, while the phase is at the edge of the area. These results present a significant difference from those obtained through the synthesis and design. Further analysis of the design is carried out to properly understand the causes of this difference. Owing to the datasheet of RO4003C suggesting two different values to design, and we have chosen the average, a study of the effect of ϵ_r in the uniform plane wave is carried out. Hence, the designed layout is analyzed for several values of ϵ_r, computing the uniform plane wave for each one. The new simulated results are compared with the measurements, finding out that for $\epsilon_r = 3.60$ we obtain the best agreement. This value is close to the maximum value provided by the RO4003C datasheet [18]. The comparison with measurements is shown in Fig. 5 for the cut $y = 0$, which is the offset plane of the reflectarray, and it is affected by the feed position. The tangent loss has been also evaluated, finding out that slight deviations of the value used in the design do not affect the uniform plane wave.

B. Evaluation of the uniform plane wave

Once the value of ϵ_r has been properly set to 3.60, the reflectarray is designed again following the method described in the previous section. The prototype is measured, and the uniform plane wave is evaluated at several planes, from 500 mm ups to 650 mm at 28 GHz. The measured offset plane of the reflectarray ($x = 0$) is shown in Fig. 6. This plane presents a higher deviation than the symmetric plane ($y = 0$) because of the feed displacement. Hence, this plane is the critical one on the uniform plane wave. For both polarization the results are quite good, showing that most of the cut is within the requirements. The taper of the amplitude increases in the further planes for both polarizations, but the maximum deviation is almost 1.7 dB in the worst case, $z = 650$ mm. This fact might be expected since no restrictions are imposed on those planes during the synthesis to keep the uniformity of the wave. Besides, other effects might appear, such as propagation. The phase presents a uniform behavior, especially at the center of the uniform plane wave wherein the phase is within the required ±5°. Moreover, only at the edge of the uniform plane wave, the phase deviation increases. It is worthy to note that the phase presents a similar response through the whole measured volume.

TABLE II: Evaluation of the maximum deviations with respect to average values and the specification compliance in the quiet zone for the starting phase distributions, optimized phase distributions and designed reflectarray for X- and Y-polarizations:

Plane (mm)		Amplitude			Phase			
		Maximum deviation (dB)	Compliance ±0.5 dB	Compliance ±0.75 dB	Maximum deviation (deg)	Compliance ±5°	Compliance ±7.5°	Compliance ±10°
500	X-pol.	**1.80**	**88.83**	**98.30**	**17.48**	**72.54**	**89.21**	**100**
	Y-pol.	**1.75**	**89.43**	**99.15**	**18.51**	**76.66**	**94.11**	**100**
550	X-pol.	**1.64**	**94.11**	**99.21**	**17.06**	**70.58**	**86.27**	**100**
	Y-pol.	**1.55**	**95.11**	**99.46**	**16.92**	**77.46**	**98.03**	**100**
600	X-pol.	**1.80**	**81.27**	**85.15**	**15.95**	**76.16**	**91.17**	**100**
	Y-pol.	**1.98**	**84.56**	**86.29**	**15.93**	**76.48**	**96.01**	**100**
650	X-pol.	**1.91**	**74.62**	**78.22**	**16.58**	**76.46**	**91.1**	**100**
	Y-pol.	**2.10**	**76.04**	**78.43**	**15.24**	**79.46**	**99.01**	**100**

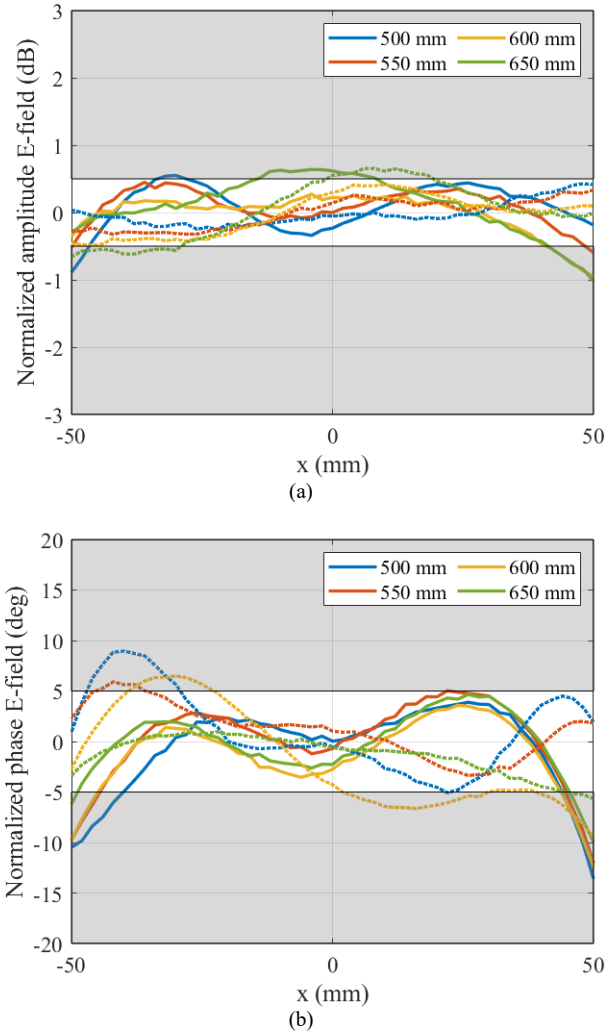

Fig. 6. Offset cut ($x = 0$) of the uniform plane wave radiated by the prototype at 28 GHz through a volume for the X- (solid lines) and (dashed lines) Y-polarization: (a) amplitude (b) phase.

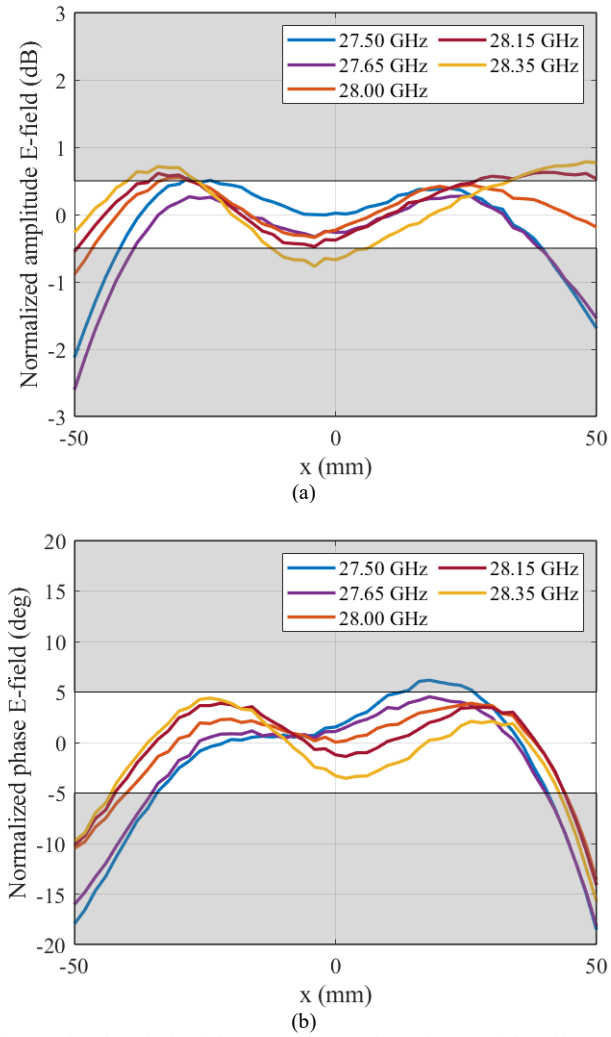

Fig. 7 In-band analysis of the 5G mm-wave channel n261 of the offset cut of the X-polarized uniform plane wave: (a) amplitude (b) phase at 500 mm.

Table II outlines the amplitude and phase response considering the whole measured area. Likewise, the offset plane, the uniform plane wave shows high compliance for both polarizations, especially at 500 and 550 mm. More than 88% of the plane wave is within ±0.5 dB of deviation, and more than 98% is within ±0.75 dB of deviation. Although the taper of amplitude increases its deviation at the further planes, the compliance is over 74.62% and 78.22% for ±0.5 dB and ±0.75 dB, respectively, for the worst case. The maximum deviation is evaluated as the maximum peak-to-peak ripple for the whole area. Although this value might seem to be over the specifications, these points are singularities found in areas close to the edge of the uniform plane wave. The phase presents a similar response through the four planes. More than 70% is within a deviation of ±5°. However, this compliance increases up to nearly 90% when a deviation of ±7.5° is evaluated. In this case, the compliance is quite similar throughout the whole volume, resulting in an extremely plane wave. Overall, the

measurements show that the reflectarray radiates an almost uniform plane wave at 500 mm and it is extended through 150 mm about $\hat{s}$.

Although the reflectarray has been designed considering a single frequency, 28 GHz, the in-band performance of the uniform plane wave has been also analyzed. Particularly, from 27.50 GHz to 28.35 GHz, covering the 5G mm-wave band n261 that is defined for mm-wave communications in 5G-NR networks. Fig. 7 shows the in-band response of the offset plane of the X-polarized uniform plane wave. According to Table II both polarizations have similar behavior, therefore only the X-polarization uniform plane wave is shown. The ripple on both amplitude and phase is almost kept within the whole band, only presenting an increase in the deviation at the edge of the area and the extreme frequencies. However, the uniform plane wave is smooth enough and the central area is similar to 28 GHz. Hence, it is expected that the reflectarray antenna can be used to characterize devices within this operational band. Out of this band, the uniform plane wave presents a higher deviation that makes the uniform plane wave unworkable. The proposed reflectarray is based on a single-frequency design, nonetheless, the in-band performance might be improved by using optimization with in-band constraints.

IV. Conclusion

A single-layer dual-polarized reflectarray is proposed to generate a dual-polarized uniform plane wave within its radiated near-field. The reflectarray acts as a dual-polarized PWG that can be used as a low-cost probe in a compact and portable CATR system for antenna characterization in the mm-wave band. The antenna is made up of two sets of orthogonal-coplanar dipoles that provides independent control of the phase shift in each polarization. To obtain a low-complex topology of the unit cell, the orthogonal-coplanar dipoles are printed in the same layer of the dielectric. Therefore, this topology offers an easy manufacturing process, as well as an ultra-thin low-profile alternative. The reflectarray is synthesized to obtain a uniform plane wave within a circular area of diameter of 100 mm (equivalent to a 56.6% of the antenna aperture) at 500 mm (46.6λ) from the center of the antenna at 28 GHz. This configuration is a quite compact structure considering that the far-field starts at 12.54 m ($\sim 1170\lambda$). Within the required circular area, the near field must present the amplitude and phase ripples within ± 0.5 dB and $\pm 5°$, respectively. The synthesis processes have improved the compliance from 16.7% to 100% in amplitude, while the phase preserves its flatness within 80% of the area. The solution obtained in this process is used to manufacture a prototype using RO4003C as the dielectric material. However, the initial measurements showed a strong deviation with simulations. A further study of the results provides a more accurate value of the dielectric constant of RO4003C. A new prototype was manufactured and measured. In this case, the measurements show a high agreement with simulations and obtained a nearly uniform plane wave at the desired distance. Besides, the uniform plane wave is also evaluated through a cylinder volume of 150 mm depth. Within this volume, the uniform plane wave almost keeps its flatness and uniformity, especially in terms of the radiated phase. Finally, the in-band response of the uniform plane wave, from 27.5 to 28.35 GHz is evaluated. This operational band corresponds to the 5G mm-wave band n261. Despite designing the reflectarray at a single frequency, the uniform plane wave presents a similar behavior in the whole band. At the extreme frequencies, the size of the uniform plane wave starts to be shortened. However, the central area shows a good response to be used in the characterization of the antenna. It should be noted that the design is carried out using a POS, thus there is no control over the in-band response of the antenna. To include the in-band response as a requirement the POS must be replaced by a more complex optimization, such as a direct optimization of the geometry of the unit cell.

References

[1] C. A. Balanis, *Antenna Theory: Analysis and Design*. Hoboken, NJ, USA: Wiley, 2005.

[2] Y. I. López, M. García-Fernández, and F. Las-Heras, "A portable cost-effective amplitude and phase antenna measurement system," in *IEEE Trans. Instrum. Meas.*, vol. 69, no. 9, pp. 7240-7251, 2020.

[3] G. Álvarez Narciandi, J. Laviada, Y. Álvarez López, and F. Las-Heras, "Portable free-hand system for real-time antenna diagnosis and characterization", in *Trans. Antennas Propag.*, vol. 68, no. 7, pp. 5636-5645, 2020.

[4] T. S. Rappaport et al., "Millimeter Wave Mobile Communications for 5G Cellular: It Will Work!," *IEEE ACCESS*, vol. 1, pp. 335-349, 2013.

[5] F. Scattone, D. Sekuljica, A. Giacomini, F. Saccardi, A. Scannavini, E. Kaverine, S. Anwar, N. Gross, P. O. Iversen, and L. J. Foged, "Towards testing of 5G millimeter wave devices using plane wave generators," in *2021 15th European Conference on Antennas and Propagation (EuCAP)*, 2021, pp. 1-4.

[6] Y. Zhang, Z. Wang, X. Sun, Z. Qiao, W. Fan, and J. Miao, "Design and implementation of a wideband dual-polarized plane wave generator with tapered feeding nonuniform array," in *IEEE Antennas Wirel.*, vol. 19, no. 11, pp. 1988-1992, 2020.

[7] D. R. Prado, A. F. Vaquero, M. Arrebola, M. R. Pino, and F. Las-Heras, "General near field synthesis of reflectarray antennas for their use as probes in CATR," in *Prog. Electromagn. Res.*, vol. 160, pp. 9-17, 2017.

[8] C. Granet, M. Zhou, S. B. Sørensen, K. W. Smart, J. S. Kot and J. Ness, "Reflectarray Compact Antenna Test Range Concept," in *2019 13th European Conference on Antennas and Propagation (EuCAP)*, 2019, pp. *1-5.*

[9] Y. Wu, J. Wu, and Z. Li, "Plane Wave Synthesis Using Near Field Wave Spectrum Transform Embedded into Intersection Approach," in *2018 International Conference on Microwave and Millimeter Wave Technology (ICMMT)*, 2018, pp. *1-3*.

[10] Á. F. Vaquero, M. Arrebola, M. R. Pino, R. Florencio, and J. A. Encinar, "Demonstration of a Reflectarray With Near-Field Amplitude and Phase Constraints as Compact Antenna Test Range Probe for 5G New Radio Devices," in *IEEE Trans. Antennas Propag.*, vol. 69, no. 5, pp. 2715-2726, May., 2021.

[11] Pozar, D.M., Targonski, S.D., Syrigos, H.D.: 'Design of millimeter wave microstrip reflectarray', *IEEE Trans. Antennas Propag*., 1997, 45, pp. 287–296.

[12] Encinar, J.A.: 'Design of two-layer printed reflectarrays using patches of variable size', *IEEE Trans. Antennas Propag*., 2001, 49, pp. 1403–1410.

[13] Encinar, J.A., Zornoza, J.A.: 'Broadband design of three-layer printed reflectarrays', *IEEE Trans. Antennas Propag*., 2003, 51, pp. 1662–1664.

[14] R. Florencio, J. A. Encinar, R. R. Boix, G. Perez-Palomino ``Dual polarisation reflectarray made of cells with two orthogonal sets of parallel dipoles for bandwidth and cross-polarisation improvement," *IET Microw. Antennas Propag*., vol. 8, pp. 1389-1397, Jun. 2014.

[15] R. Florencio, J. A. Encinar, R. R. Boix, V. Losada, and G. Toso, "Reflectarray antennas for dual polarization and broadband telecom satellite applications," *IEEE Trans. Antennas Propag*., vol. 63, no. 4, pp. 1234–1246, Apr. 2015.

[16] D. Martinez-De-Rioja, E. Martinez-De-Rioja, J. A. Encinar, R. Florencio, and G. Toso, "Reflectarray to generate four adjacent beams per feed for multispot satellite antennas," *IEEE Trans. Antennas Propag*., vol. 67, no. 2, pp. 1265–1269, Feb. 2019.

[17] A. F. Vaquero, D. R. Prado, M. Arrebola, M. R. Pino, and F. Las-Heras, "Near field synthesis of reflectarrays using Intersection Approach," in *Proc. 11st Eur. Conf. Antennas Propag. (EuCAP)*, Paris, France, Mar. 19-24, 2017.

[18] Rogers Corporation. Available online: https://rogerscorp.com (accessed on 6 Oct 2021).

[19] R. Florencio, R. R. Boix, E. Carrasco, J. A. Encinar, and V. Losada, "Efficient numerical tool for the analysis and design of reflectarrays based on cells with three parallel dipoles", *Microw. Opt. Technol. Lett*., vol. 55, no. 6, pp. 1212–1216, June 2013.

[20] J. Huang and J. A. Encinar, *Reflectarray antennas*. Piscataway, NJ/New York: IEEE Press/Wiley, 2008.

[21] D. R. Prado, M. Arrebola, M. R. Pino, and G. Goussetis, "Contoured-Beam Dual-Band Dual-Linear Polarized Reflectarray Design Using a

Multiobjective Multistage Optimization," *IEEE Trans. Antennas Propag.*, vol. 68, no. 11, pp. 7682–7687, Nov. 2020.